Digital holographic microscopy for the cytomorphological imaging of cells under zero gravity

Toy, M. Fatih, Richard, Stephane, Kühn, Jonas, Franco-Obregón, Alfredo, Egli, Marcel, et al.

M. Fatih Toy, Stephane Richard, Jonas Kühn, Alfredo Franco-Obregón, Marcel Egli, Christian Depeursinge, "Digital holographic microscopy for the cytomorphological imaging of cells under zero gravity," Proc. SPIE 8227, Three-Dimensional and Multidimensional Microscopy: Image Acquisition and Processing XIX, 82270S (2 February 2012); doi: 10.1117/12.908413

SPIE.

Event: SPIE BiOS, 2012, San Francisco, California, United States

Digital holographic microscopy for the cytomorphological imaging of cells under zero gravity

M. Fatih Toy[*a], Stephane Richard[b], Jonas Kühn[c], Alfredo Franco-Obregón[b], Marcel Egli[b], Christian Depeursinge[a]
[a]École Polytechnique Fédérale de Lausanne (EPFL), Advanced Photonics Laboratory, CH-1015, Lausanne, Switzerland;
[b]Eidgenössische Technische Hochschule Zurich, Space Biology Group, CH-8005, Zurich, Switzerland;
[c]École Polytechnique Fédérale de Lausanne (EPFL), Biomolecular Screening Facility, CH-1015, Lausanne, Switzerland;

ABSTRACT

Digital holographic microscopy (DHM) has been gaining interest from cell biology community because of its label free nature and quantitative phase signal output. Besides, fast shutter time, image reconstruction by numerical propagation of the wave fields, and numerical compensation of the aberrations are other intrinsic advantages of this technique that can be explored for harsh imaging conditions. In the frame of this work, a transmission type DHM is developed with a decoupled epifluorescence microscopy mode for cytomorphological monitoring under zero gravity and hyper gravity. With the implemented automatic post processing routines, real time observation of the cell morphology is proven to be feasible under the influence of mechanical disturbances of zero gravity platforms. Post processing of holograms is composed from dynamic numerical compensation of holograms, robust autofocusing and phase image registration. Experiments on live myoblast cells are carried out on two different platforms; random positioning machine (RPM), a ground base microgravity simulation platform, and parabolic flight campaign (PFC), a fixed wing plane flight providing short durations of alternating gravity conditions. Results show clear perinuclear phase increase. During seconds scale microgravity exposure, measurable scale morphological modifications are observed with the accumulated effect of repetitive exposures and short breaks.

Keywords: microscopy, holography, digital holographic microscopy, fluorescence microscopy, microgravity, cell morphology, cytoskeleton

1. INTRODUCTION

This work essentially focuses on to develop a microscope operating both in Digital Holographic Microscopy (DHM) and wide field fluorescence microscopy modes and to utilize this microscope for the observation of microgravity induced cytoskeletal modifications on myoblast cells. Accessibility of microgravity platforms for biological studies is the key factor to reach the goals of this work. Random Positioning Machine (RPM), Parabolic Flight Campaigns (PFC), Sounding Rockets, and High Altitude Balloon Drops are the microgravity simulation platforms that are suitable for such a biological study. Among these, RPM, a computer controlled system of two randomly rotating concentric frames that accommodate biological sample at the center of the inner frame, has its own advantages as being easily accessible ground base simulation platform and large experiment volume. Because of these reasons, first version of the microscope was realized based on the specs of RPM. Initially the microscope was developed and customized; and preliminary experiments were carried out [1-3]. After this step, mechanical design of the microscope was optimized for parabolic flight requirements, and developed system took place in the ESA 53rd Parabolic Flight Campaign for further experimentation. In this paper a hologram post processing methodology adapted for such a challenging mechanical environment discussed and supported with results from live cell experiments from both platforms.

Three-Dimensional and Multidimensional Microscopy: Image Acquisition and Processing XIX, edited by Jose-Angel Conchello, Carol J. Cogswell, Tony Wilson, Thomas G. Brown, Proc. of SPIE Vol. 8227, 82270S · © 2012 SPIE · CCC code: 1605-7422/12/$18 · doi: 10.1117/12.908413

2. METHODS AND EXPERIMENTAL SETUP

Digital holography enables the numerical reconstruction of a complex field emerging from an object from a recorded hologram of the object on a digital camera. Reconstructed complex object field includes both the absorption and optical path variation information of the object in the full field [4]. This optical path information can be a function of the sample's topology in reflection or optical thickness, axially integrated refractive index, in transmission type of recording. In off-axis recording, a small angle exists between the propagation directions object and reference waves captured on the camera. Spatial modulation arising from the tilt angle yields to the separation of object wave related information from others which can be filtered in spectrum [5]. Any aberration can be easily compensated by the numerical lenses [6]. On the application side, DHM in transmission mode holds a great potential for the non-invasive marker free imaging of 3D cell morphology with the advantage of speed and digital refocusing over other methods [7].

Microscope capable of time sequential DHM and widefield epi-fluorescence microscopy mode is mechanically fixed on the inner RPM frame. For the first operation mode, laser beam from a laser diode is split into two arms using a beam splitter (BS) and expanded form of an arm reaches to dichroic beamsplitter in filter cube (FC). The other one is incident on cell sample (S) through a condenser lens (CL), and forms the image of the sample on Andor Luca electron multiplying CCD (EMCCD) camera located at the image plane of 60X microscope objective (MO). Interference of the arms forms the hologram on the camera. In the fluorescence microscopy mode, a light emitting diode (LED) with the emission spectrum overlapping to the excitation spectra of EGFP transfected actin filaments in C2C12 cells acts as the excitation source. Illumination shape of the excitation source is controlled by a lens and a diaphragm on the excitation path. Shaped excitation reaches to the cell sample through the filter cube and microscope objective and emitted fluorescence signal is imaged on the. Figure 1shows the 3D model of the microscope housing and optical scheme.

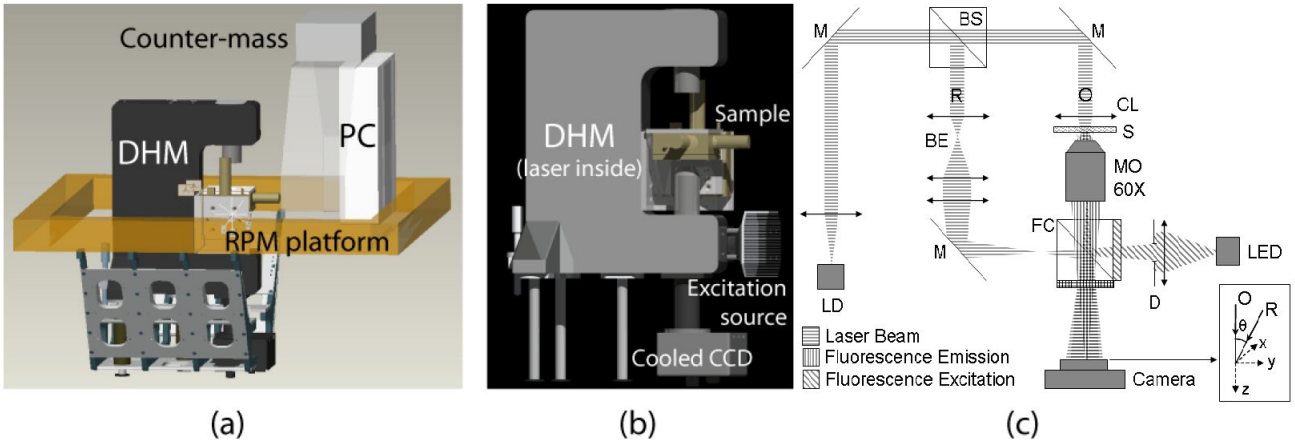

Figure 1 Upgraded RPM DHM with fluorescence imaging channel. (a) 3D rendering of the system mounted on the RPM, with its standing frame, on-board mini-PC and electronics, and a counter-mass to equilibrate torques; (b) RPM-DHM 3-D rendering, showing the fluorescence excitation source and the fluorescence-sensitive cooled CCD camera; (c) Internal optical setup schematic.

Rotation of the RPM frames during microgravity simulation and resulting shocks cause elastic displacement of the sample stage and tilt of beams. This displacement is observed as the loss of focus and change of imaging field of view on the CCD camera. As an extremely important advantage of DHM, we can numerically propagate the captured holograms, so in this way it is possible to solve this issue. In case of a single hologram, phase images are observed by an operator for different propagation distances to find the best focus distance. However, in scope of this work every experiment involves capturing of several thousand holograms. Since it is not possible to manually process this amount of holograms, eventually it is required to implement an auto-focusing algorithm. Primary consideration for the implementation is the computational cost (execution time) of the chosen approach. Golden section search is chosen as the optimization approach to minimize the number of iterations to reach the best focus propagation. This unimodal approach is quite sensitive to errors, and requires the optimization parameter to be free of local extremities. Variance and gradient of the propagated field's amplitude [8] are compared based on their shape; this comparison is shown in the graph in Figure 2. This graph shows the behavior of these optimization parameters as propagation distance changes. In contrast to amplitude variance, its gradient counterpart experiences oscillations on the general trend reaching to an extremity at the correct propagation distance. Because of this reason, amplitude variance over a central region is chosen as the

optimization parameter. With some tweaks on the implementation side, auto-focusing code is realized in Matlab environment with an execution time at second scale.

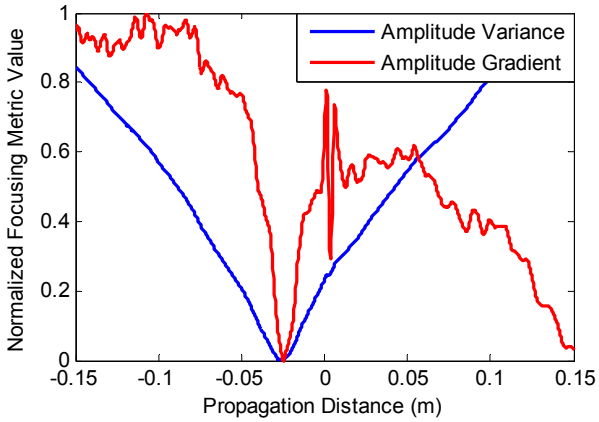

Figure 2 Graph showing the comparison of chosen auto-focusing parameters as a function propagation distance for an experimental hologram

Another side effect of the aforementioned elastic displacement of sample holder is the change of the camera field of view on the sample. Correction for this change is also carried out in the post processing step after the auto-focusing. Phase images from the auto-focused fields are transferred to an image registration code [9].

With these software side improvements, microscope has been in use on RPM for different experimental conditions. All experiments with the live cells are carried in a temperature regulated room at 37°C. In the first phase, experiments are mainly carried out using EGFP Actin transfected mutant C2C12 mouse myoblast cells with a control in 1g condition. Experimental protocol has been standardized to include a fixed duration of DHM and Fluorescence channel acquisitions in 1g with a single fluorescence image acquisition after 9 DHM channel acquisitions. After this control period, RPM is started to rotate at 60°/sec to simulate microgravity conditions and acquisitions are continued with the same settings for an hour. This microgravity simulation phase is interrupted at every five minutes for the acquisition of a fluorescence mode image with no focus loss.

Furthermore, microscope developed in the scope of this work took place with some modifications at the 53rd ESA parabolic flight campaign in October 2010. Safety interlocking of laser with warning light and a containment box are installed on DHM to meet with safety requirements of the campaign. Another addition to microscope is a heating subsystem. A passive heater was mounted on the sample holder to keep the cells at the optimum temperature range. Parabolic flight campaigns involve three flight days with 31 parabolic maneuvers of the plane at every flight. Single parabola of the plane is illustrated in Figure 3 with 20 seconds of hypergravity phase in which gravity has a value between 1.5g and 1.8g. A microgravity phase of 20 seconds with 10^{-2}g follows this hypergravity phase, and maneuver ends with another hypergravity phase.

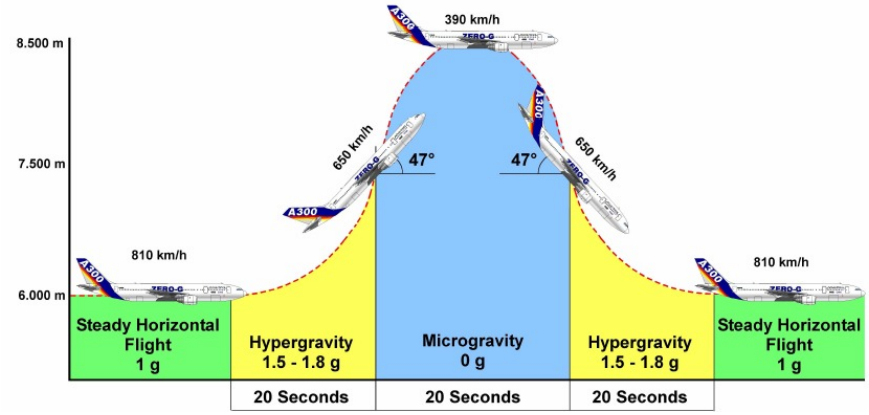

Figure 3 Single parabola of the parabolic flight illustrated with the corresponding gravity values and periods

This parabolic flight campaign gave us the chance to test entire system for parabolic flight conditions. Based on the performance of microscope and identification of other subsystem requirements in this campaign, microscope will be further developed for a specific type of experiment to take place in future campaigns. Following figure shows the assembled system on the rack before flight (left) and entire system during operation in plane (right).

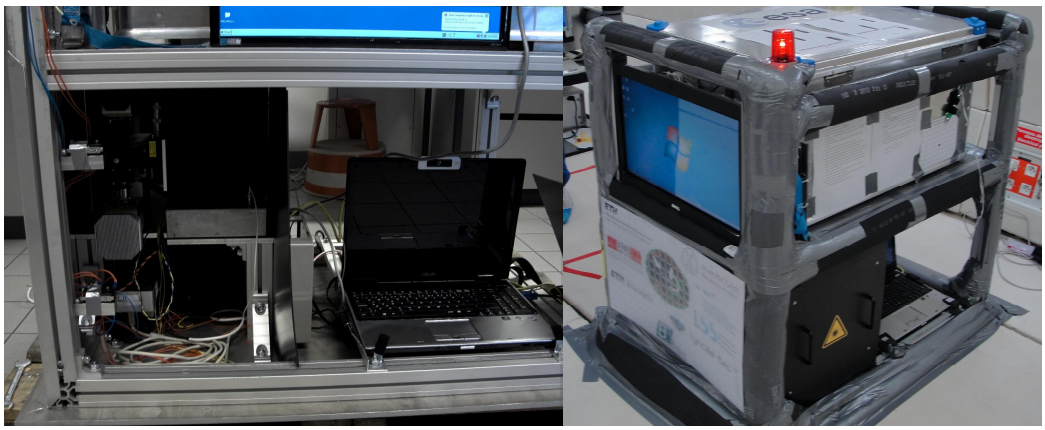

Figure 4 Parabolic Flight Campaign rack with the DHM installed at the lower shelf. Close up view with the front door removed (left) and overall view of the rack (right).

3. RESULTS

Experiments on RPM have yielded to interesting early results, experiments indicated to a cellular response in the order of minutes under microgravity conditions. More interestingly, mean perinuclear phase shows a slow recovery characteristic with the reloading of gravity. Data from a cell showing this type of behavior is shown in Figure 5. This specific cell is exposed to ground level gravity conditions for 5 minutes to have a short control measurement. Then the cell is exposed to simulated microgravity. In this part of the experiment, cellular response starts around after few minutes and phase shows and increasing behavior that indicates to the migration of intracellular material.

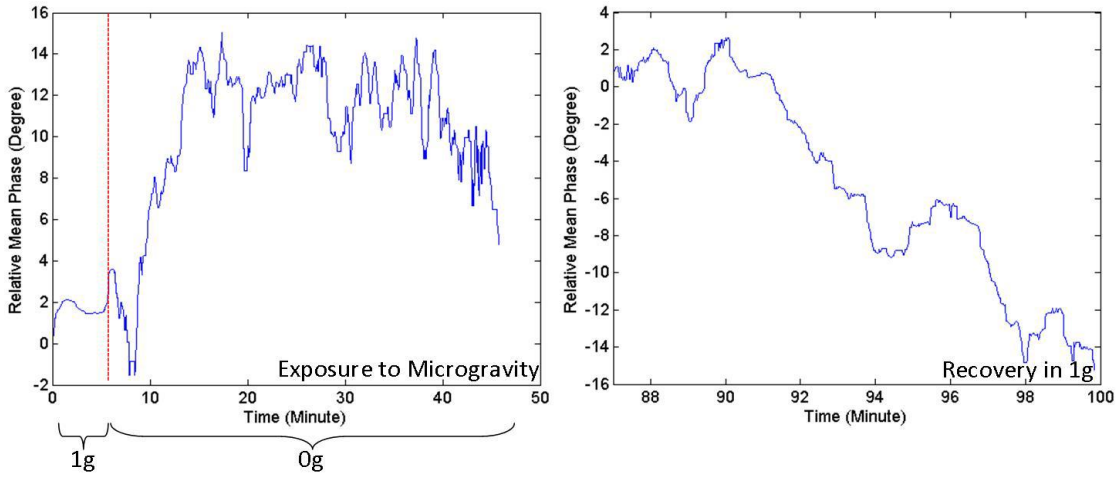

Figure 5 Mean phase of a C2C12 mouse myoblast cell in time. Phase stays stable in the control of 5minutes in 1g. With the exposure to simulated microgravity, it increases and gets stabilized (Left). A slow recovery of phase is observed after returning back to 1g condition (Right).

As the second part of the experiments, a representative result from the parabolic flight campaign is given in Figure 6. This figure shows the variation of phase from the perinuclear region of a cell during four parabolas. Left y axis of this graph references to the blue dashed line representing the magnitude of longitudinal g. Green trace is perinuclear phase signal with the y axis reference on the right hand side. As it can be observed from the figure, this perinuclear phase signal has a continuously increasing behavior with the parabolas.

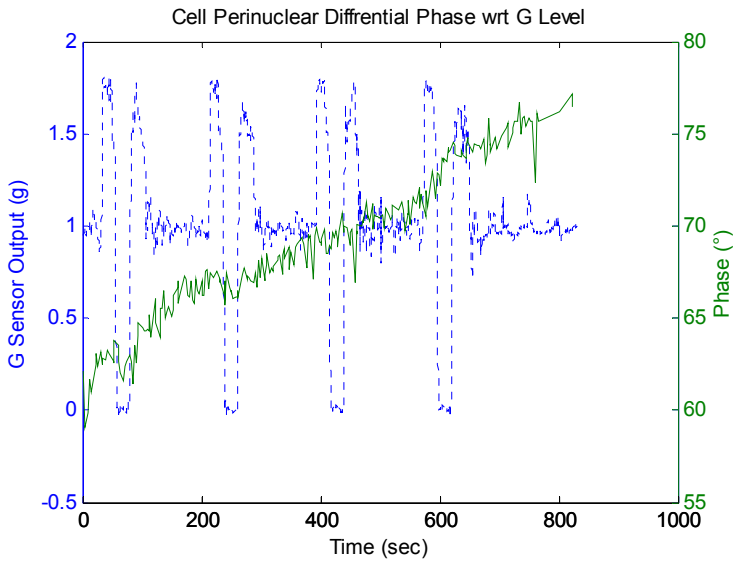

Figure 6 Perinuclear phase increase of a cell with four sequential parabolas.

4. CONCLUSIONS

A time sequential dual mode microscope capable of DHM and widefield epi-fluorescence operations is realized and optimized for two microgravity platforms, RPM and PFC, for cytomorphological imaging. In spite of the operation in such extreme conditions, inherent advantages of DHM supported with post processing algorithms for hologram autofocusing and image registration enables microscope operation. Live cell experiments carried out on RPM and PFC indicates to cytomorphological modification.

ACKNOWLEDGEMENTS

The authors would like to thank to EPFL Space Research Programme (ESRP) for its financial support, Lyncée tec (www.lynceetec.com) for their technical help and fruitful discussions, ESA and Novespace for the participation opportunity to 53rd Parabolic Flight Campaign and their campaign support.

REFERENCES

[1] Pache C., Kühn J., Westphal K., Toy M. F., Parent J., Büchi O., Franco-Obregón A., Depeursinge C., and Egli M., "Digital holographic microscopy real-time monitoring of cytoarchitectural alterations during simulated microgravity", J. Biomed. Opt. 15, 026021 (2010).

[2] Toy M. F., Pache C., Parent J., Kühn J., Egli M., and Depeursinge C., "Dual-mode digital holographic and fluorescence microscopy for the study of morphological changes in cells under simulated microgravity" Three-Dimensional and Multidimensional Microscopy: Image Acquisition and Processing XVII, volume 7570, page 75700A, San Francisco CA, January 23-28, 2010 (2010).

[3] Toy M. F., Kühn J., Parent J., Pache C., Egli M., and Depeursinge C., "Real Time 3-D Cytomorphological Imaging Using Digital Holographic Microscopy and Fluorescence Microscopy for Space Biology", Digital Holography and Three-Dimensional Imaging (DH), page DTuA5, Miami, FL, USA, April 12-14, 2010 (2010).

[4] Cuche E., Marquet P. and Depeursinge C., "Simultaneous amplitude-contrast and quantitative phase-contrast microscopy by numerical reconstruction of Fresnel off-axis holograms". Appl. Opt. 38, 6994–7001 (1999).

[5] Cuche E., Marquet P. and Depeursinge C., "Spatial filtering for zero-order and twin-image elimination in digital off-axis holography," Appl. Opt. 39, 4070-4075 (2000).

[6] Colomb T., Cuche E., Charrière F., Kühn J., Aspert N., Montfort F., Marquet P., and Depeursinge C., "Automatic procedure for aberrations compensation in digital holographic microscopy and applications to specimen shape compensation". Appl. Opt. 45, 851–863 (2006).

[7] Marquet P., Rappaz B., Magistretti P., Cuche E., Emery Y., Colomb T., and Depeursinge C., "Digital holographic microscopy: a noninvasive contrast imaging technique allowing quantitative visualization of living cells with subwavelength axial accuracy", Optics Leters, 30, 468-470 (2005).
[8] Langehanenberg P., Kemper B., Dirksen D., and von Bally G., "Autofocusing in digital holographic phase contrast microscopy on pure phase objects for live cell imaging," Appl. Opt. 47, D176-D182 (2008).
[9] Guizar-Sicairos M., Thurman S. T., and Fienup J. R., "Efficient subpixel image registration algorithms," Opt. Lett. 33, 156-158 (2008).